Theoretical investigation on co-sensitization of natural dyes for dye sensitized solar cells (dsscs) applications

1*MASUA A J., 1MWANGA S., 1PAMAIN S A., 2BABU N S., 1LYIMO J E, 1LAXMIKANTH

1Department of Physics, The University of Dodoma, Dodoma, Tanzania
2Department of chemistry, The University of Dodoma, Dodoma, Tanzania

Corresponding Author: masuaanthony850@gmail.com

Abstract

This study reports the effect of co-sensitization of four dye molecules of 3,5,7-trihydroxy-2-(4-hydroxy-3-methoxyphenyl) chromen-4-one, 2-phenylchromen-4-one, betalains, and 2-descarboxy-betanidin from *Senna singueana* leaves, *Begonia malabarica* leaves, *Bougainvillea glabra* bract, and *Celosia cristata* flowers, respectively, for dye-sensitized solar cell applications. Co-sensitization was done by designing new dyes (D1, D2, and D3) by attaching molecules M2, M3, and M4 to molecule (M1). Moreover, the optimized molecular structures of the individuals and newly designed dyes were investigated through density functional theory (DFT) and time-dependent density functional theory (TD-DFT) calculations by using the GAUSSIAN 09 software package. The results on newly designed dyes as sensitizers on DSSC showed a reduction in the HOMO-LUMO energy gap compared to the individual dyes. The newly co-sensitized dye molecules (D1, D2, and D3) were reported to have energy gap (E_g) of 2.29, 2.73, and 1.91 eV, respectively, which was very small compared to individual molecules (M1, M2, M3, and M4) with an energy gap of 2.88, 2.70, 3.12, and 2.34 eV respectively. Additionally, the maximum absorption spectra were extended up to 849.55 nm for newly dye D3 compared with 683.96 nm for the individual dye M4. Furthermore, the highest light harvesting efficiency (LHE) was changed from 0.5829 for individual dye (M1) up to 0.9582 for newly dye (D3). Thus, the energy band gap (E_g), the light harvesting efficiency (LHE), and absorption spectra of the newly designed dyes were enhanced compared to individual dyes. However, among the newly designed dyes, D3 showed the best properties compared to D1 and D2 for dye-sensitized solar cell applications.

Cite as, *Masua et al., (2024)*. Theoretical investigation on co-sensitization of natural dyes for dye sensitized solar cells (dsscs) applications. *East African Journal of Science, Technology and Innovation 6(Special issue 1).*

Introduction

The rapid increase in worldwide energy demand and the depletion of readily available fossil fuels call for the need of energy sources that are ecological, affordable, and more cost effective than conventional fossil fuel sources. Thus, there is a great need to search for alternative sources of energy. Dye sensitized solar cells (DSSC) represent a promising third generation solar technology that is environmentally friendly and has a low production cost (Pandey *et al.*, 2022). DSSC consists of a working electrode, counter electrode, sensitizer (dye), and redox electrolyte as the main components (Sharma, Sharma and Sharma, 2018). Among these components, dye

plays a crucial role in absorbing and converting sunlight into electrical energy. However, the performance of DSSC is still low and unstable, greatly influenced by dyes and semiconductor electrodes (Daniel, Baby and Manoj, 2021).

Various, attempts have been made to overcome these challenges, including the discovery of new stable dyes with good absorption, the use of solid electrolytes, the purification of dyes, and the co-sensitization of two or more dyes (Kusumastuti, Anis and Rozana, 2022). Moreover, different research has been made to develop many sensitizers; such as quantum-dot sensitizers, perovskite sensitizers, metal-based complex dyes, metal-free organic dyes, mordant dyes, and natural dyes (Ammar *et al.,* 2019). Nevertheless, metal complexes and organic dyes have been produced and used as sensitizers (Sanjay, Isaivani, Deepa, Madhavan and Senthil, 2019). However, the power conversion efficiency of 14% has been attained through ruthenium-metal complexes based DSSC (Kenji Kakiage *et al.,*2015). Though, the highest efficiency of ruthenium-metal complexes has been reached, its limitations are high costs of production and toxicity (Andualem and Demiss, 2018). On the other hand, metal-free organic dyes attained efficiency of 11% to 12% and do not pose any threat to the environment compared to the metal complex (Pandey *et al.,* 2022). However, the main challenge lies in the complex and costly synthesis method required to extract these dyes (Amelia, Sawitri and Risanti, 2023). Furthermore, natural dyes extracted from some parts of plants, such as fruits, flowers, leaves, and roots represent a very attractive alternative to metal based complex and free metal dyes. However, natural dyes suffer from low efficiency and instability (Ossai, Ezike, Timtere and Ahmed, 2021).

Moreover, researchers are working on the discovery of new dyes, optimizing the thickness of photo anodes and co-sensitization for enhancing the efficiency and stability of dyes in DSSCs. For instance, Sakalani *et al.,* (2022) reported an efficiency of 0.68% and 0.45% for *Senna singueana* leaves and *Bougainvillea glabra bract*; Hosseinnezhad *et al.,* (2018) reported efficiencies of 1.38%, 0.52%, 1.12%, and 0.65% for *Celosia cristata*, saffron, *cynoglossum,* and *eggplant peel* and Singh and Koiry *et al.,* (2018) reported an

efficiency of 1.76% for *Begonia malabarica* leaves. For co-sensitization, an efficiency of 0.56% was obtained compared to a single sensitizer with efficiencies of 0.25% and 0.29% for black cherry fruits and *Carica papaya* leaf, respectively (Ossai *et al.,* 2021). Also, co-sensitization of chlorophyll and anthocyanin sensitizers gave the highest conversion efficiency of 1.63% compared to individual efficiencies of 0.4% and 0.31%, respectively (Emmanuel, Donald and Ikhioya, 2022). Furthermore, the co-sensitization of *Celosia cristata* and *cynoglossum* resulted in an efficiency of 2.32% (Hosseinnezhad, Rouhani and Gharanjig, 2018), thus, it is evident that the co-sensitization of dyes enhances the performance of dyes. It is worth noting that these results are experimental one.

Thus, theoretical studies are essential in supplementing and enhancing experimental investigations (Ndiaye *et al.,* 2021). Likewise, it helps the researchers to provide better exploration of electronic, photovoltaic, and optical absorption properties of natural dyes (Subbarao, 2023). Therefore, this study was intended to use a theoretical approach to investigate the effectiveness of co-sensitization of natural dye for DSSC applications from *Senna singueana* leaves, *Begonia malabarica* leaves, *Bougainvillea glabra bracts*, and *Celosia cristata* flowers. Furthermore, the electronic properties, photovoltaic properties, and absorption properties of dye molecules were calculated through density functional theory (DFT) and time-dependent density functional theory (TD-DFT) calculations.

Materials and Methods

The structures of several dyes, including3,5,7-trihydroxy-2-(4-hydroxy-3-methoxyphenyl)chromen-4-one (M1), 2-phenylchromen-4-one (M2), betalains (M3), and 2-descarboxy-betanidin (M4), were sketched by using chem Draw software (Figure 1a). The optimization calculations of dye molecular structures at their ground state were carried out by using the density functional theory (DFT) calculation method with B3LYP functional and 6-311G basis sets in both gas-phase and ethanol solvent environments. Additionally, the HOMO and LUMO energy levels of the dye molecules in their

excited state, along with their absorption spectra, were calculated using the time- dependent density functional theory (TDDFT) at the B3LYP with basis set 6-311G for both gas-phase and ethanol solvent conditions. Finally, the geometry optimization of the four dyes (M1, M2, M3, and M4) was performed using the Gaussian 09 software, and the resulting optimized structures are shown in Figure 1b in the gas-phase and ethanol-solvent environments.

After optimization, it was observed that all these four dyes (M1, M2, M3, and M4) were suitable candidates to be used as sensitizers in DSSC.

However, the dye molecule M1, derived from the *Celosia cristata* flower plant, exhibited the best harvesting ability in both gas-phase and ethanol solvent conditions. Therefore, a co-sensitization approach was adopted, where the molecule M1 was kept constant and the other dye molecules (M2, M3, and M4) were attached to M1 to create the new dye molecules D1, D2, and D3 respectively (Figure 1c). Similarly, the geometry optimization of three newly designed dyes (D1, D2, and D3) was then carried out using the Gaussian 09 software, and the optimized structures are presented in Figure 1d for both the gas-phase and ethanol-solvent environments.

Figure 1

(a) The molecular structure of dyes M1, M2, M3, and M4 from senna singueana leaves, begonia malabarica leaves, bougainvillea glabra bract, and celosia cristata flowers, respectively (b) Optimized molecular structure of dyes before co-sensitization in both gas-phase and ethanol-solvent (c) The molecular structure of the newly designed dyes (D1, D2 and D3) (d) Optimized molecular structure of dyes molecules after co-sensitization in both gas-phase and ethanol-solvent.
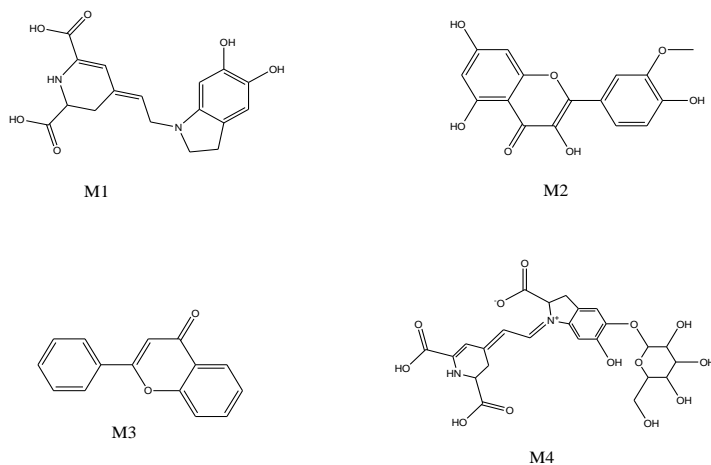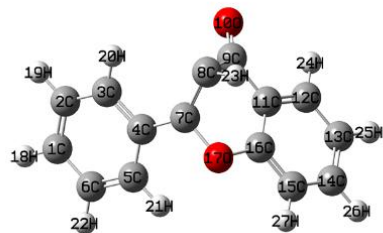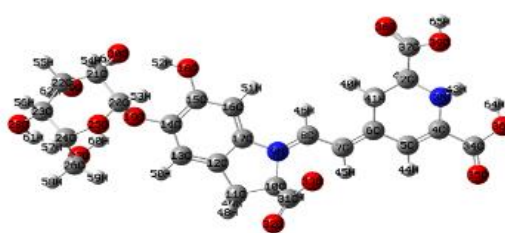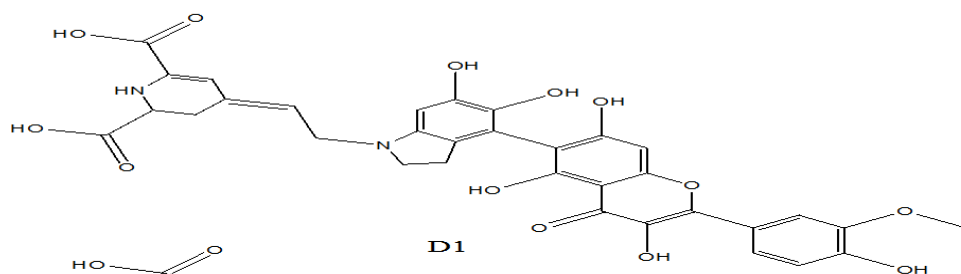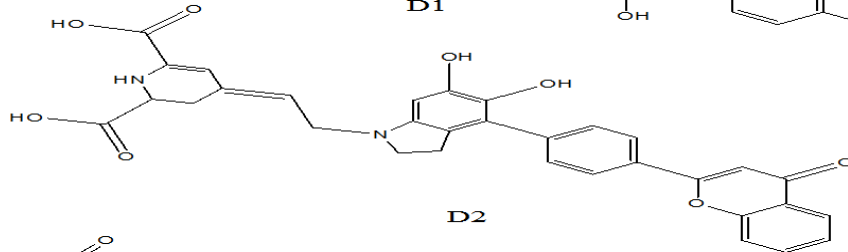

(a)
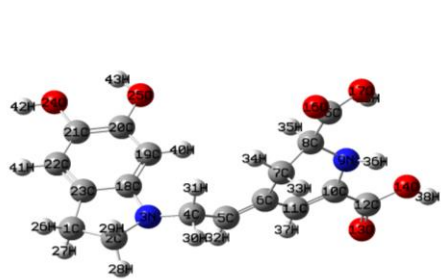
M1
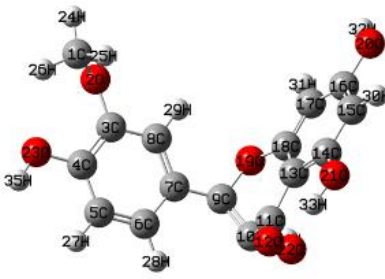
M2

M3

M4

(b)

D1

D2

D3

(c)

D1

D2

D3
(d)

5
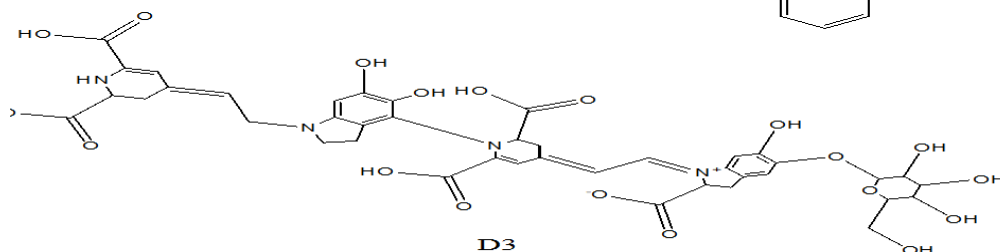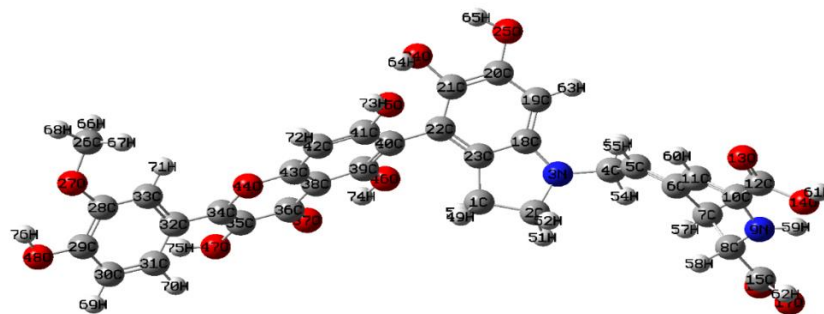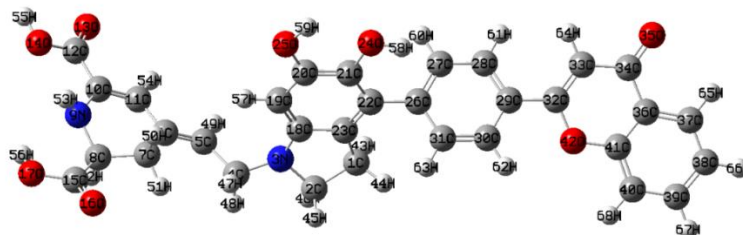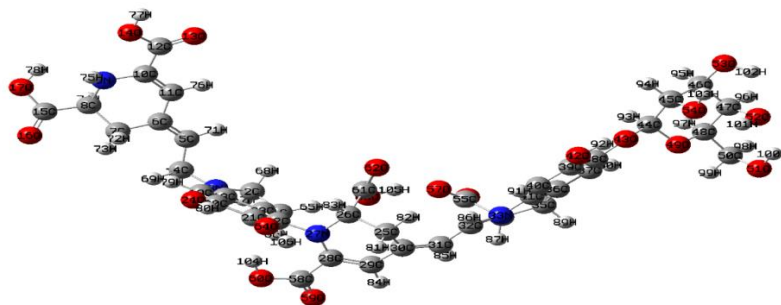
Figure 2

Frontier molecular orbitals of dyes molecules in gas phase (b) Frontier molecular orbitals of dyes molecules under the effect of ethanol solvent (c) Frontier molecular orbitals of co-sensitized dyes molecules in gas phase (d) Frontier molecular orbital of co-sensitized dye molecules under the effect of ethanol solvent

M1-HOMO   M1-LUMO

M2-HOMO   M2-LUMO

M3-HOMO   M3-LUMO
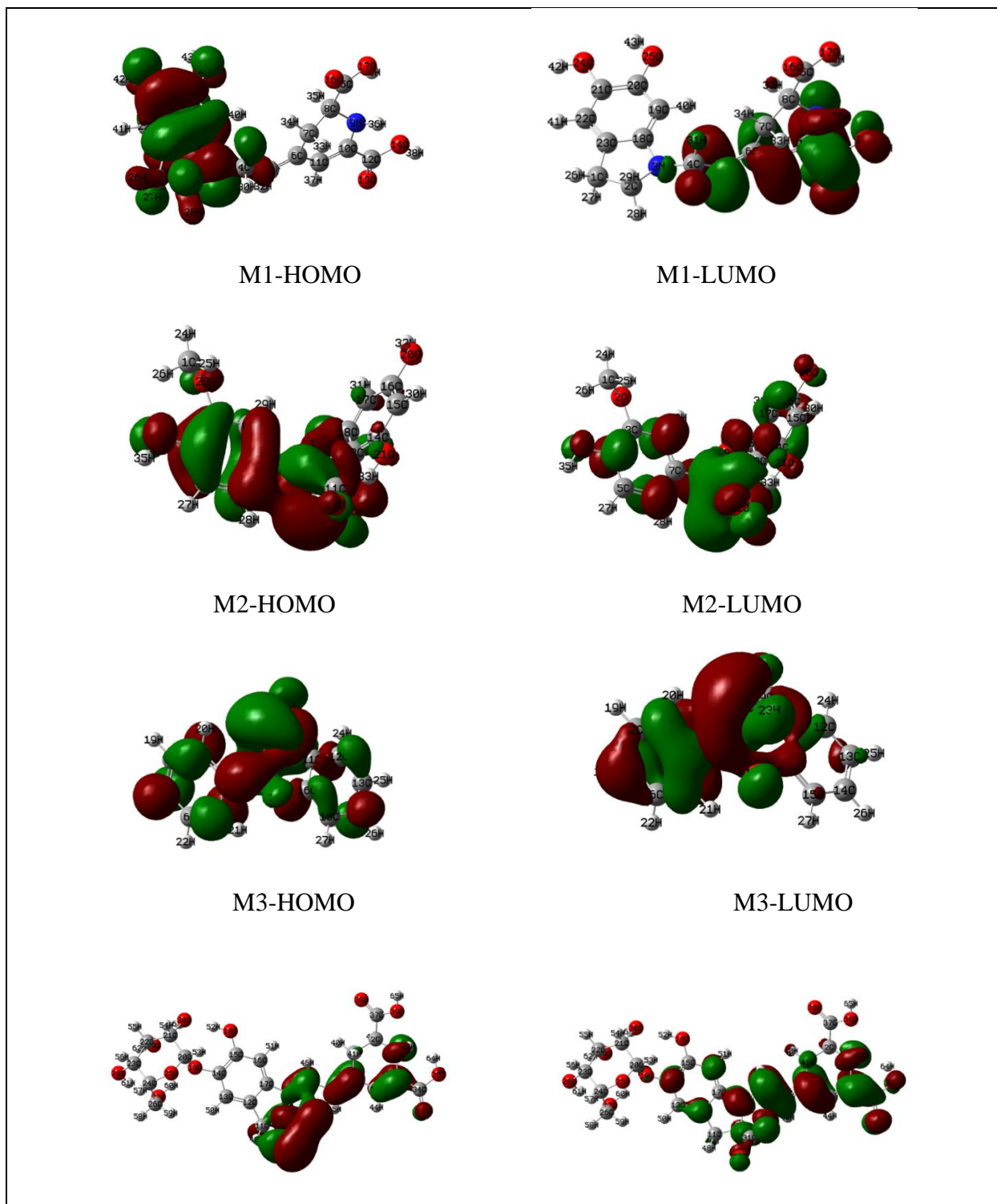
M4-HOMO	M4-LUMO

(a)

M1-HOMO

M1-LUMO

M2-HOMO

M2-LUMO

M3-HOMO

M3-LUMO

M4-HOMO

M4-LUMO

(b)
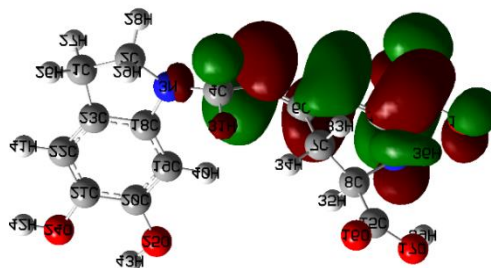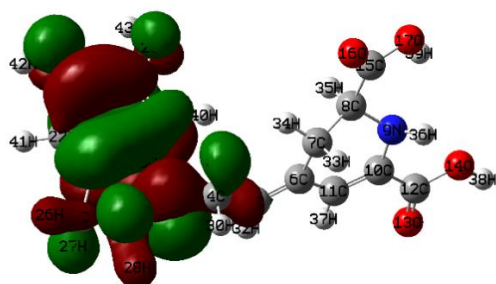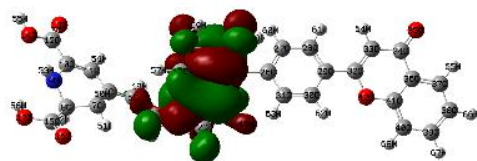
D1-HOMO
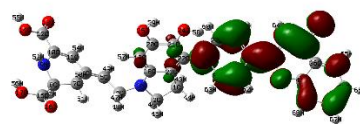
D1-LUMO

D2-HOMO   D2-LUMO

D3-HOMO   D3-LUMO

(c)

D1-HOMO   D1-LUMO

D2-HOMO   D2-LUMO

	D3-HOMO	D3-LUMO

(d)
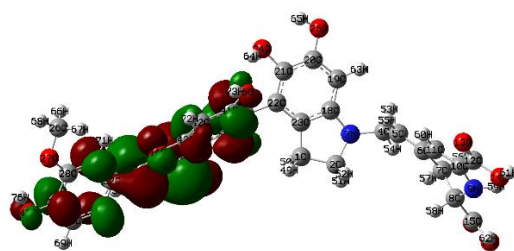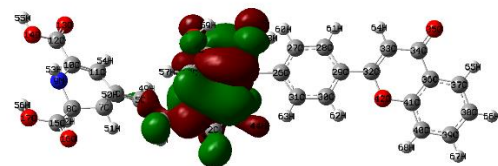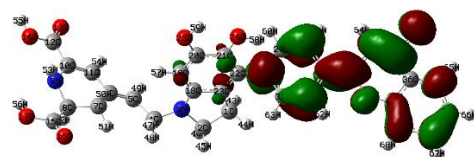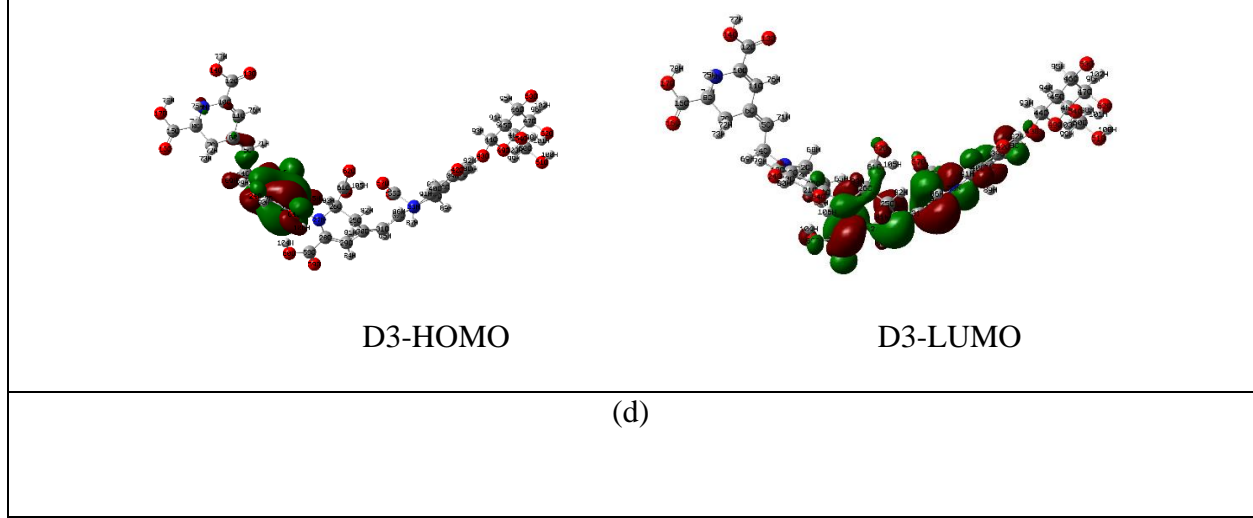
Different parameters that influence the electrical performances of DSSCs, including energy gap (E_g), light harvesting efficiency (*LHE*), free energy of injection (ΔG^{inject}), electron regeneration energy (ΔG^{regen}), open-circuit voltage (V_{oc}), oxidation energy of the dye in the ground state (E^{dye}), and oxidation energy of the dye in the excited state (E^{dye*}) were calculated using Equations 1 – 7, respectively:
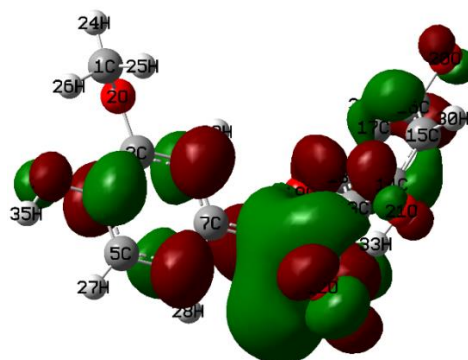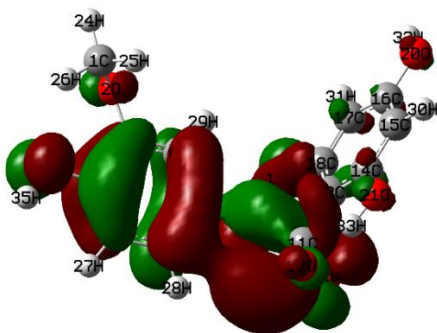
$$E_g = E_{HOMO} - E_{LUMO} \qquad (1)$$

$$LHE = 1 - 10^{-f} \qquad (2)$$

$$\Delta G^{inject} = e^{dye*} + E_{CB} \qquad (3)$$

$$E^{dye*} = E^{dye} - E^{00} \qquad (4)$$

$$\Delta G^{regen} = E^{dye} + E_{redox} \qquad (5)$$

$$E^{dye} = -E_{HOMO} \qquad (6)$$

$$V_{OC} = E_{HOMO} - E_{CB} \qquad (7)$$

Where, E_{HOMO} and E_{LUMO} are the highest and lowest energies occupied molecular orbitals respectively, f is the oscillator strength relatively to the maximum absorption wavelength (λ_{nm}), E^{dye*} represents the oxidation potential energy of molecules in the excited state, and E_{CB} represents the reduction potential of the conduction band of TiO$_2$, whose value is –4.0 eV (Ndiaye *et al.*, 2021). Other parameters are E^{dye} oxidization potential energy at the ground state and E^{00} is vertical electronic transition energy. E_{redox} is the redox potential of the electrolyte, whose value is -4.8 eV (Babu and Vuai, 2021).
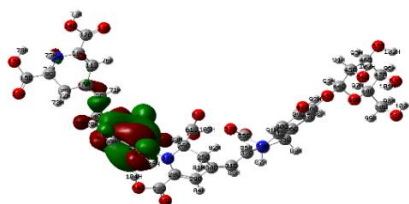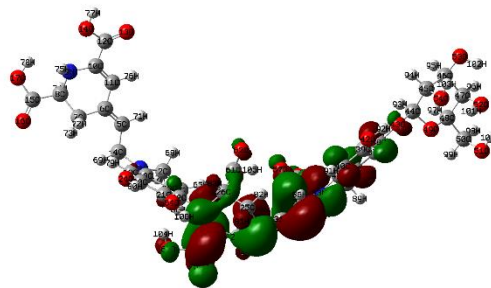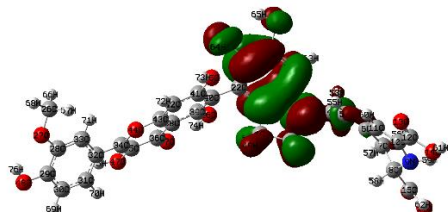
Results

Analysis of frontier molecular orbitals (fmos) of the dye molecules
Frontier molecular orbitals (FMOS) show how the dye molecules' highest occupied molecular orbital (HOMO) and lowest unoccupied molecular orbital (LUMO) relate to each other. The HOMO represents the highest energy level that contains electrons, while the LUMO represents the lowest energy level that lacks an electron (Hilal, Aziz, Osman and Bredas, 2017). These two parameters influence the dye molecules photo-excitation process.

Furthermore, HOMO represents the bonding character, while LUMO represents the antibonding character. Figures 2a and 2b describe the results of electrons density before co-sensitization in both gas-phase and ethanol solvents. In Figures 2c and 2d resulted the electronic density after co-sensitization of dyes in both gas-phase and ethanol solvent.

Electronic properties

The electronic properties of dye molecules are crucial as they determine the efficiency and stability of DSSCs (Subbarao, 2023). These properties include the highest occupied molecular orbital (HOMO), the lowest unoccupied molecular orbital (LUMO) energy level, and the band gap energy. The HOMO-LUMO energies are important parameters for understanding if the charge transfer between the donor and acceptor will occur or not. The energy levels for HOMOs of dye molecules M1, M2, M3,

and M4 are −5.052, −5.667, −6.003, −5.830, and −5.044, −5.731, −6.158, and −6.013 eV for gas-phase and ethanol solvent, respectively. In addition, the corresponding energies of LUMOs of M1, M2, M3, and M4 are −2.173, −2.964, −2.882, −3.487, and −2.152, −3.105, −3.062, −3.435 eV for gas-phase and ethanol solvent respectively. The energy gaps of the dyes were calculated using Equation 1, and the results are presented in Tables 1 and 2 for both gas-phase and ethanol solvents.

Table 1

HOMO-LUMO energies of co-sensitized dye molecules in the gas phase.

Dye	HOMO (eV)	LUMO (eV)	Energy gap (E_g) (eV)
D1	-4.77858	-2.48629	2.29229
D2	-5.19056	-2.46099	2.7296
D3	-5.4479	-3.5339	1.914

Table 2

HOMO-LUMO energies of co-sensitized dye molecules in ethanol solvent

Dye	HOMO (eV)	LUMO (eV)	Energy Gap (E_g) (eV)
D1	-5.0466	-2.4417	2.6049
D2	-5.1198	-2.4577	2.6621
D3	-5.362	-3.4308	1.9312

Photovoltaic properties

The performance of dye-sensitized solar cells (DSSCs) can be evaluated by considering several key photovoltaic parameters, including light harvesting efficiency (*LHE*), negative free energy of injection (ΔG^{inject}), electron regeneration energy (ΔG^{regen}), open-circuit voltage (V_{oc}),

oxidation energy of the dye in the ground state (E^{dye}), and oxidation energy of the dye in the excited state (E^{dye*}). These parameters were calculated using Equations 3–7, and the results for these photovoltaic parameters are presented in Tables 3 and 4, for the dye molecules in both gas-phase and ethanol solvents, respectively.

Table 3

The photovoltaic properties of dye molecules in the gas phase.

Dye	E^{00}	E^{dye}	E^{dye*}	ΔG^{inject}	ΔG^{regen}	LHE	V_{oc}
M1	2.3752	5.05205	2.67685	-1.32315	0.25205	0.5553	1.8269
M2	2.3219	5.6673	3.3454	-0.6546	0.8673	0.4218	1.03587
M3	2.6735	6.00336	3.32986	-0.67014	1.20336	0.1137	1.11832
M4	1.8128	5.83084	4.01804	0.01804	1.03084	0.5653	0.5126

Table 4

The photovoltaic properties of dye molecules under the effect of ethanol solvent.

Dye	E^{00}	E^{dye}	E^{dye*}	ΔG^{inject}	ΔG^{regen}	LHE	V_{oc}
M1	2.3835	5.04471	2.66121	-1.33879	0.24471	0.5829	1.84786
M2	2.2075	5.73125	3.52375	-0.47625	0.93125	0.322	0.89464
M3	2.6054	6.15847	3.55307	-0.44693	1.35847	0.1469	0.93737
M4	2.245	6.01343	3.76843	-0.23157	1.21343	0.0310	0.56403

For the co-sensitization, the results of photovoltaic parameters were changed compare to those before co-sensitization. The results of new designed dyes D1, D2, and D3 in both gas phase and solvent are tabulated in Tables 5 and 6.

Table 5

The photovoltaic properties of co-sensitized dye molecules in the gas phase.

Dye	E^{00}	E^{dye}	E^{dye*}	ΔG^{inject}	ΔG^{regen}	LHE	V_{oc}
D1	1.8759	4.77858	2.90268	-1.09732	-0.0214	0.0135	1.51371
D2	2.3049	5.19056	2.88566	-1.11434	0.39056	0.00871	1.53901
D3	3.3929	5.4479	2.055	-1.945	0.6479	0.9582	0.4661

Table 6

The photovoltaic properties of co-sensitized dye molecules under the effect of ethanol solvent.

| Dye	E^{00}	E^{dye}	E^{dye*}	ΔG^{inject}	ΔG^{regen}	LHE	V_{oc}
D1	2.1831	5.0466	2.8635	-1.1365	0.2466	0.0164	1.5583
D2	2.2574	5.1198	2.8624	-1.1376	0.3198	0.0092	1.5423
D3	2.3274	5.362	3.0346	-0.9654	0.562	0.8869	0.5692

Optical absorption properties

The absorption parameters, which include the oscillator strength (f), maximum absorption wavelength, and vertical transition energy, indicate the ability of the dye molecules to absorb light. These parameters were determined using Equation 2. The optical absorption spectra of those dyes showed maximum absorption wavelengths of M1, M2, M3, and M4 at 521.99, 533.97, 463.75, and 683.96 nm with respect to the oscillator strengths of 0.352, 0.2379, 0.0524, and 0.3618, respectively, in the gas phase. In ethanol solvent, the results of maximum absorption peaks for dyes M1, M2, M3, and M4 were 520.18, 561.65, 475.88, and 552.28 nm, with respect to oscillator strengths of 0.3798, 0.1688, 0.0765, and 0.0137, respectively. However, after co-sensitization, the results changed for the newly designed dyes D1, D2, and D3 for both maximum wavelengths and oscillator strengths that were 660.94, 537 and 365.42 nm, with corresponding oscillator strength of 0.043, 0.004 and 1.378 respectively in gas phase. While in the ethanol solvent, the maximum absorption wavelengths of D1, D2, and D3 were 567.94, 549.23, and 849.55 nm, with oscillator strengths of 0.207, 0.007 and, 0.947, respectively. Figures 3a and 3b depict the absorption spectra of dyes M1, M2, M3, and M4 dye molecules, while Figures 4 and 5 illustrate the effect of co-sensitization on the newly dyes in both the gas-phase and ethanol solvent.

Figure 3

(a) UV-Vis absorption spectra obtained for the dye molecules via the output of TDDFT calculations in gas phase (b) UV-Vis absorption spectra obtained for the dye molecules via the output of TDDFT calculations under the effect of ethanol-solvent.
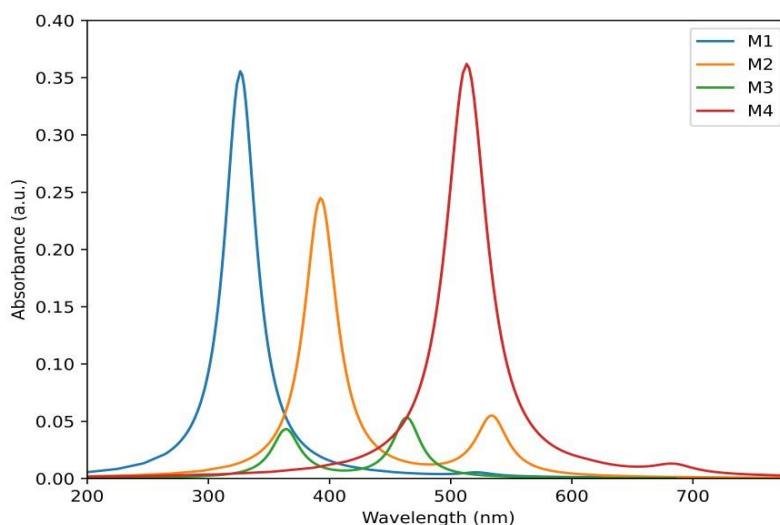
(a)
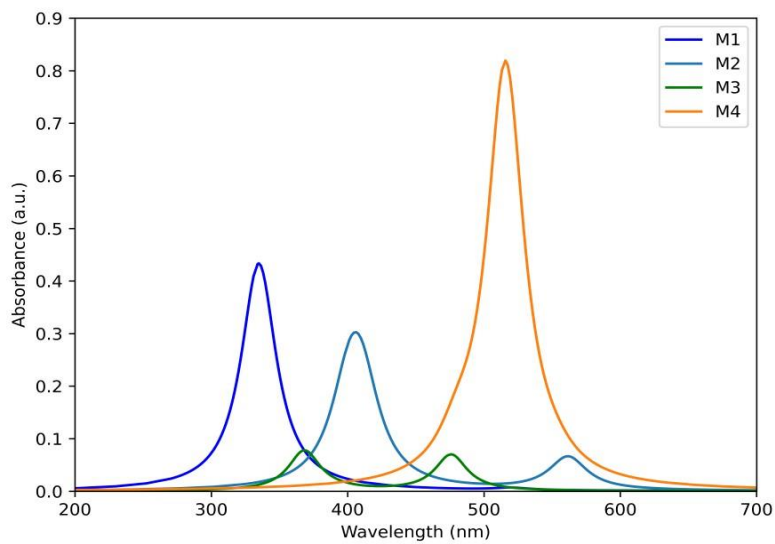
(b)

Figure 4

UV-Vis absorption spectra obtained for the newly designed dye molecules (a) D1=M1+M2, (b) D2=M1+M3 and (c) D3=M1 +M4 via the output of TD-DFT calculations in gas phase.

Figure 5

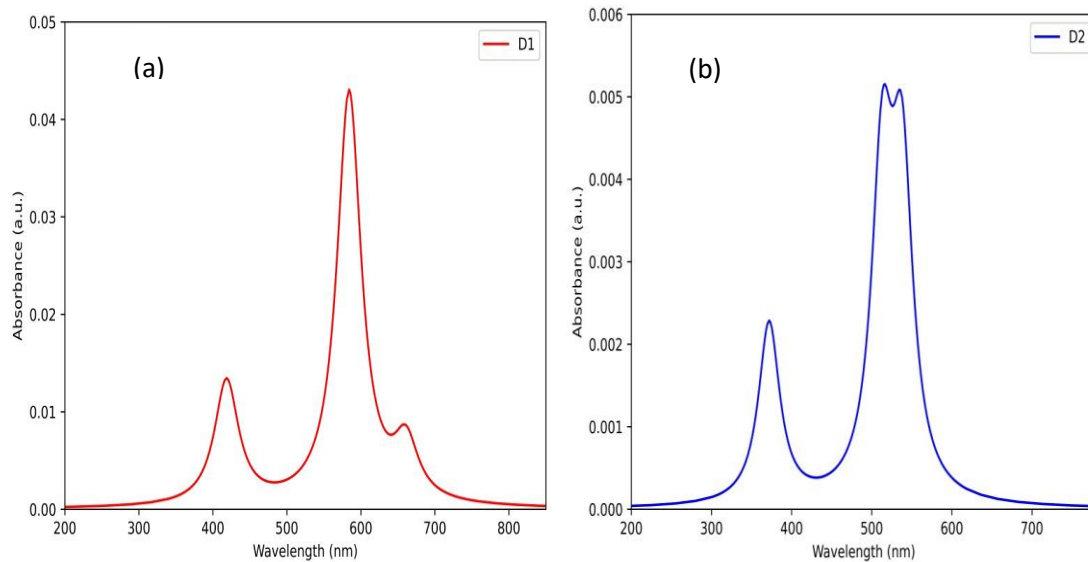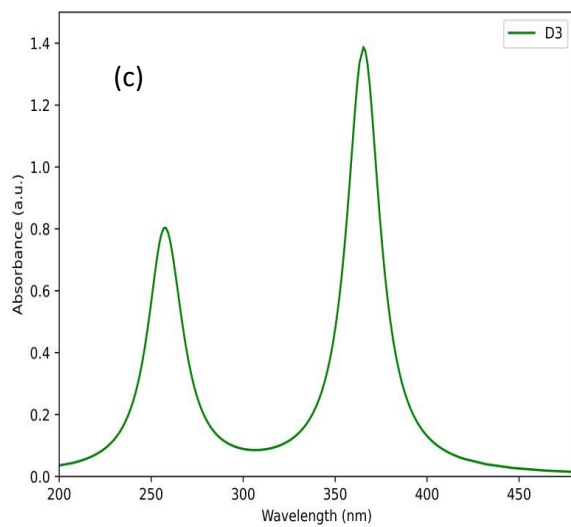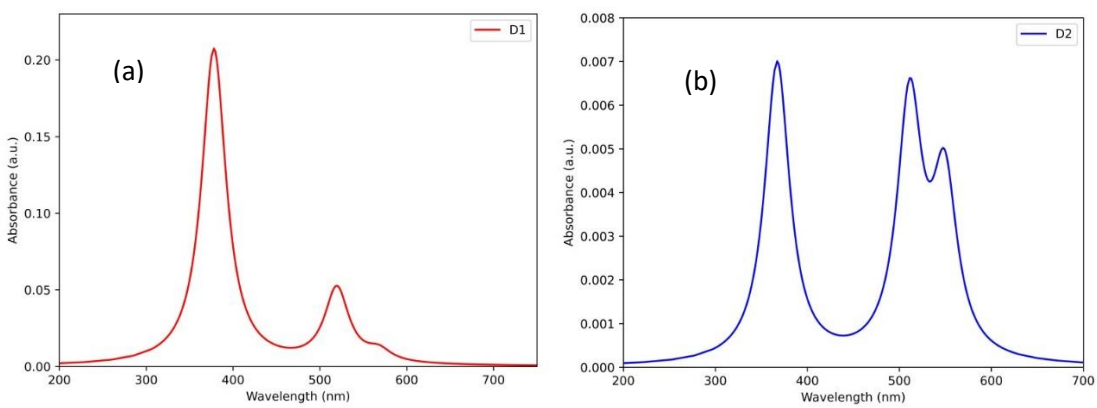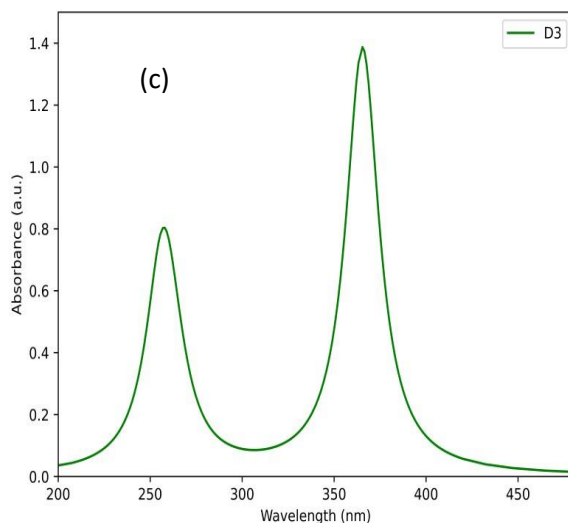*UV-Vis absorption spectra obtained for the newly dye molecules (a) D1=M1+M2, (b) D2=M1+M3 and (c) D3=M1+M4 via the output of TDDFT calculations under the effect of ethanol solvent*

(c)

Discussion

From Figures 2a and 2b, it was observed that the HOMO orbitals are localized on the donor parts of the dye molecules, while the LUMO orbitals are generally found on the acceptor parts, which is similar to the results of Gunawardhana *et al.*, (2024). Additionally, Figures 2a and 2b display an optimal overlap between the HOMO and LUMO for some of the dye molecules (M3 and M4). These make the four dye molecules suitable candidates for use in DSSC since they have the ability to eject electrons into the conduction band of TiO₂. The dye molecule M1 was well localized in both HOMO and LUMO compared to dye molecules M2, M3, and M4. This resulted -in the better electronic charge transfer characteristics of M1 than the other three molecules in both the gas phase and the ethanol solvent which is comparable to other findings (Dey, Sreenivasulu, Veerendra, Rao and Babu, 2022). While after the co-sensitization process, the newly designed dye molecules exhibited a higher level of localization in the donor part of the HOMO compared to the acceptor part of the LUMO (Figures 2c and 2d). This suggests that there is a greater intermolecular transfer of electrons from the dye molecules to the conduction band of the TiO₂ semiconductor material, as reported by (Babu and Vuai, 2021).

For dye-sensitized solar cell (DSSC) applications, the HOMO energy level of the dye should be lower than the redox couple potential (I^- / I_3^-) of the electrolyte, which is −4.8 eV (Păuşescu *et al.*, 2022). Additionally, the LUMO energy level of the dye molecule should be higher than the conduction band of titanium dioxide (TiO₂), which is −4.0 eV (Huam, Celestino and Quintana, 2021). The results of the HOMO and LUMO energy values of the four dye molecules satisfied these required conditions for them to be used as sensitizers in DSSC applications. This suggests that the four dye molecules derived from *Senna singueana* leaves, *Begonia malabarica* leaves, *Bougainvillea glabra bracts*, and *Celosia cristata* flowers are suitable candidates for DSSC applications. In addition, the dye molecule M1 exhibited the highest LUMO energy level of −2.152 eV among the four dye molecules studied. The higher the LUMO energy level of the dye molecule, the more effectively it injects electrons into the conduction band of TiO₂, which has an energy level of −4.0 eV (Huam *et al.*, 2021). However, among the newly designed dye molecules, D2 and D3 have the lowest HOMO energy levels, which are lower than the redox couple potential (I^- / I_3^-)-of the electrolyte at -4.8 eV (Vuai, Khalfan and Babu, 2021). Conversely, the HOMO energy of the new dye molecule D1 is higher than the redox couple potential, meaning it does not satisfy this requirement. As a result,

the new dye molecule D1 will likely fail to efficiently receive electrons from the redox couple potential of the electrolyte, limiting the regeneration process of the oxidized D1 dye molecule comparable to results of (Jaafar, Minggu, Arifin, Kassim and Wan, 2017).

Moreover, the energy band gaps (E_g) of these dye molecules are still relatively high compared to that of the semiconductor material. For optimal DSSC performance, the energy gap of the dye molecules should be similar to that of a semiconductor material, as suggested by Kantesaria (2014) and Syafinar, Gomesh, Irwanto, Fareq and Irwan (2015). This is because a smaller energy gap can enhance the efficiency of dye injection and the short-circuit current (J_{sc}) of the DSSC device (Lyakurwa and Numbury, 2023). Specifically, the dye molecule M4 exhibited the lowest energy gap of 2.343 eV in the gas phase and 2.577 eV in the ethanol solvent, compared to the other dye molecules (M1, M2, and M3). Therefore, electron transfer can take place easily for M4 compared to M1, M2, and M3 because of the energy gap value (Hosseinnezhad *et al.*, 2018). Furthermore, the energy band gaps of the newly designed dye molecules (D1, D2, and D3) in Tables 3 and 4 were reduced compared to the individual dye molecules as presented in Tables 1 and 2. It is worth noting that the energy band gap of D3 was the smallest, with values of 1.914 eV in the gas phase and 1.931 eV in the ethanol solvent, than dyes D1 and D2. The reduction in the energy gap of the dye molecules facilitates an increase in electron transfer from the HOMO to the LUMO levels, as explained by (Lyakurwa and Numbury, 2023). Consequently, this lead to an increase in the short-circuit current density as well as the power conversion efficiency of the DSSC device (Subbarao, 2023).

For optimal DSSC performance, the light harvesting efficiency (*LHE*) should be maximized, as a higher *LHE* promotes greater photocurrent generation. The *LHE* is directly correlated with the oscillator strength - the higher the oscillator strength, the higher the *LHE*, which in turn leads to improved injection of electrons and a slightly higher short-circuit current for the dye molecules (Munusamy *et al.*, 2021). From the results presented in Tables 3 and 4, the dye molecule M1 exhibited the highest *LHE* in both

the gas and ethanol solvents compared to others. Still, the dye molecule M1 had an oscillator strength of 0.352 in the gas phase, but this value increased to 0.3798 in the ethanol solvent. This was the maximum oscillator strength value observed across both the gas and ethanol solvents, indicating that the dye molecule M1 has the highest ability to interact with light and absorb the maximum amount of light. Based on these findings, the dye molecule M1 is recommended as a suitable candidate for DSSC applications as compared with other results (Galappaththi, Lim, Ekanayake and Petra, 2017). Furthermore, the *LHE* values were observed to increase after the co-sensitization of the dye molecules as indicated in Tables 5 and 6. Notably, the newly designed dye molecule D3 was found to have the highest *LHE* among the tested dyes in both the gas and ethanol solvent. The results showed that prior to co-sensitization, the highest light harvesting efficiency was 0.5829, and after co-sensitization effect, value increased significantly to 0.9582. This indicates that the ability of the dye molecules to absorb light was substantially enhanced through the co-sensitization process. Additionally, the effects of co-sensitization on the dye molecules were found to increase the oscillator strength value. For the dye molecule D3, the oscillator strength reached a high value of 1.3787 in the gas phase. Also, the polarity of the ethanol solvent caused this value to change to 0.9466, which was not observed for the individual dye molecules. In general, DSSC applications propose the dye molecule D3 as a good sensitizer candidate due to its high light absorption capability.

The free energy of injection ΔG^{inject} is another important parameter that can be used to increase the short-circuit current (J_{sc}) of the dye molecules in DSSCs. Based on the results presented in Tables 3 and 4, all the ΔG^{inject} values are negative, except for the dye molecule M4 in the gas phase. However, in the ethanol solvent, all the dye molecules exhibit more negative ΔG^{inject} values, indicating that the excited states of these dye molecules lie above the conduction band of the TiO$_2$ semiconductor (Babu and Vuai, 2021). The dye M4 attains the maximum value of free energy of injection in ethanol solvent, compared to those M1, M2, and M3. From these results, we can see that the dye molecule M4 can easily inject

17

electrons to the TiO$_2$ material's conduction band (Jaafar *et al.,* 2017). Furthermore, after the co-sensitization effect, as shown in Tables 5 and 6, all the newly designed dye molecules became more negatively charged in both the gas phase and the ethanol solvent. Notably, the dye molecule D3 in the ethanol phase was found to have the most negative ΔG^{inject} value compared to the dye molecules D1 and D2. Thus, the dye molecule D3 is considered the most suitable sensitizer for DSSC applications, as stated elsewhere (Sreeja and Pesala, 2018). Moreover, the results tabulated in Tables 3 and 4 show that the dye molecule M3 has the greatest value of the electron regeneration efficiency (ΔG^{regen}) in both the gas-phase and ethanol solvents, compared to the other dye molecules. This large ΔG^{regen} value indicates that the M3 dye can be regenerated more frequently, which in turn can lead to an increase in the short-circuit current (J_{sc}) of the DSSC, similar results are presented by (Babu and Vuai, 2021). Furthermore, after the co-sensitization process, the newly designed dye molecule D3 exhibited the highest electron regeneration efficiency value in both the gas-phase and ethanol solvent, outperforming the dye molecules D1 and D2.

The results presented in Tables 3 and 4, the dye molecule M1 exhibits the highest open-circuit voltage (V_{oc}) in both the gas-phase and ethanol solvent. The open-circuit voltage is directly proportional to the power conversion efficiency of a DSSC device (Vuai *et al.,* 2021). The combination of the high LUMO energy level and the high open-circuit voltage suggests that the dye molecule M1 would be the most preferred choice for DSSC applications among the investigated dye molecules. Furthermore, the effect of co-sensitization on both the gas-phase and ethanol solvents shows that the values of open-circuit voltage remain high for the dye molecules with higher LUMO energy levels. After the co-sensitization process, the newly designed dye molecules D1 and D2 have demonstrated higher open-circuit voltage values compared to the dye molecule D3.

In Figures 3a, 3b, 4, and 5 it was observed that the absorption spectra were changed due to the effect of the ethanol solvent as compared to the gas phase. This suggests that the ethanol solvent has an effect of advancing the absorption capabilities of the sensitizers, which can enhance the performance of DSSCs (Adedokun, Sanusi and Awodugba, 2018). From the literature, dye molecules with higher optical absorption wavelengths can absorb light with longer wavelengths, which corresponds to lower photon energies (Kumara, Lim, Lim, Petra and Ekanayake, 2017). Additionally, from Figures 3a and 3b, the dye molecules, M2 and M4, exhibited the longest absorption wavelengths in both the gas-phase and ethanol solvents. However, the absorption spectra of the dye molecules were observed to change after the effect of co-sensitization. Specifically, the absorption bands of the individual dye molecules were broadened, extending from the visible to the near-infrared regions. For the individual dye molecules, the longest absorption wavelength was 683.96 nm, observed in both the gas phase and ethanol solvent. After co-sensitization, the newly designed molecule D3 achieved a broader absorption wavelength of 849.55 nm, as presented in Figures 4 and 5. This extended absorption range of D3 demonstrates its improved capability to absorb a broader spectrum of light and promote the excitation of electrons to the LUMO level (Chalkias, Loizos and Papanicolaou, 2020). This extended absorption range for the D3 molecule is beneficial, as it can lead to more efficient photoelectric power conversion in DSSC applications compared to the individual dye molecules (Shah, Faraz, Arshad, Haider and Sayyad, 2023). The results clearly demonstrate the effects of co-sensitization were manifested in the enhanced electronic, photovoltaic, and optical absorption properties of all the investigated dye molecules.

Conclusion

A computational study was conducted to investigate the effectiveness of co-sensitizing natural dye molecules for DSSC applications. The analysis of the electronic parameters revealed that after co-sensitization, the dye molecule D3 exhibited the lowest energy band gap of 1.9 eV in both the gas phase and under the influence of the ethanol solvent. In contrast, before co-sensitization, the energy band gap values for the

individual dye molecules were higher, at 2.3 eV in the gas phase and 2.6 eV in the ethanol phase. Furthermore, the light harvesting efficiency (LHE) for the single dye molecule was observed to be 0.5829 before co-sensitization, but this value increased significantly to 0.9582 after the co-sensitization process. Additionally, the maximum absorption wavelength shifted from 683.96 nm for the individual dye molecule to 849.55 nm for the newly designed dye molecule D3 after co-sensitization. These results collectively suggest that the co-sensitization approach is an effective method for enhancing the efficiency of natural dyes for DSSC applications. Based on these findings, the newly designed dye molecule D3 appears to be a promising candidate for DSSC devices. However, to confirm these results, further experimental studies are recommended to be carried out.

References

Adedokun, O., Sanusi, Y. K., & Awodugba, A. O. (2018). Optik Solvent dependent natural dye extraction and its sensitization e ff ect for dye sensitized solar cells. *Optik - International Journal for Light and Electron Optics*, *174* (June), 497–507. https://doi.org/10.1016/j.ijleo.2018.06.064

Amelia, R., Sawitri, D., & Risanti, D. D. (2023). *used to enhance light harvesting capability*. (January 2015). https://doi.org/10.1117/12.2078268

Ammar, A. M., Mohamed, H. S. H., Yousef, M. M. K., Abdel-hafez, G. M., Hassanien, A. S., & Khalil, A. S. G. (2019). *Dye-Sensitized Solar Cells (DSSCs) Based on Extracted Natural Dyes*. *2019*.

Andualem, A., & Demiss, S. (2018). *Review on Dye-Sensitized Solar Cells (DSSCs)*. *1*(1), 29–34.

Babu, N. S., & Vuai, S. A. H. (2021). Theoretical studies of optoelectronic and photovoltaic properties of D – A polymer monomers by Density Functional Theory (DFT). *Designed Monomers and Polymers*, *24*(1), 226–239. https://doi.org/10.1080/15685551.2021.1956209

Chalkias, D. A., Loizos, D. D., & Papanicolaou, G. C. (2020). *Evaluation and prediction of dye-sensitized solar cells stability under different accelerated ageing conditions*. *207*(June), 841–850.

Daniel, P., Baby, R., & Manoj, N. (2021). *Natural Dyes from Ornamental Plants as Sensitizers for Dye-Sensitized Solar Cells (DSSCs): A Review on the Structure-Activity Relationships (SARs) between Power Conversion Effi ciencies and Chemical Constituents*. *94*(12), 1561–1576. https://doi.org/10.1134/S107042722112 0016

Dey, S., Sreenivasulu, A., Veerendra, G. T. N., Rao, K. V., & Babu, P. S. S. A. (2022). Innovation and Green Development Renewable energy present status and future potentials in India : An overview. *Innovation and Green Development*, *1*(1), 100006. https://doi.org/10.1016/j.igd.2022.100006

Emmanuel, O. C., Donald, O. N., & Ikhioya, I. L. (2022). *Effect of Doping and Co-sensitization on the Photovoltaic Properties of Natural Dye-sensitized Solar Cells*. *9*(3), 44–54.

Galappaththi, K., Lim, A., Ekanayake, P., & Petra, M. I. (2017). *Cyanidin-Based Novel Organic Sensitizer for Efficient Dye-Sensitized Solar Cells : DFT / TDDFT Study*. *2017*.

Gunawardhana, P., Balasooriya, Y., Kandanapitiye, M. S., & Chau, Y. C. (2024). *applied sciences Optoelectronic Characterization of Natural Dyes in the Quest for Enhanced Performance in Dye-Sensitized Solar Cells : A Density Functional Theory Study*.

Hilal, R., Aziz, S. G., Osman, O. I., & Bredas, J. (2017). *Time dependent – density functional theory characterization of organic dyes for dye-sensitized solar cells*. *7022*(June). https://doi.org/10.1080/08927022.2017.13

32409

Hosseinnezhad, M., Rouhani, S., & Gharanjig, K. (2018). Opto-Electronics Review Extraction and application of natural pigments for fabrication of green dye-sensitized solar cells. *Opto-Electronics Review*, *26*(2), 165–171. https://doi.org/10.1016/j.opelre.2018.04.004

Huam, A. A., Celestino, M. R., & Quintana, E. (2021). *Theoretical and experimental study of solar cells based on nanostructured fi lms of TiO 2 sensitized with natural dyes extracted from Zea mays and Bixa orellana*. 9086–9097. https://doi.org/10.1039/d1ra01043c

Jaafar, S. N. H., Minggu, L. J., Arifin, K., Kassim, M. B., & Wan, W. R. D. (2017). Natural dyes as TIO2 sensitizers with membranes for photoelectrochemical water splitting: An overview. *Renewable and Sustainable Energy Reviews*, *78*(May), 698–709. https://doi.org/10.1016/j.rser.2017.04.118

Kantesaria, S. (2014). *Optimization of dye-sensitized solar cells (DSSCs) through co-adsorption and tri-adsorption of organic dyes*. *1*(1), 13–18. https://doi.org/10.1511/CTNR.2014.1.13

Kenji Kakiage *et al*.2015. (n.d.). *ChemComm*. https://doi.org/10.1039/x0xx00000x

Kumara, N. T. R. N., Lim, A., Lim, C. M., Petra, M. I., & Ekanayake, P. (2017). Recent progress and utilization of natural pigments in dye sensitized solar cells: A review. *Renewable and Sustainable Energy Reviews*, *78*(May), 301–317. https://doi.org/10.1016/j.rser.2017.04.075

Kusumastuti, A., Anis, S., & Rozana, M. (2022). *Natural Dyes Utilization and Production Technology for Dye-Sensitized Solar Cell*. *2*(2), 154–167.

Lyakurwa, M., & Numbury, S. B. (2023). *DFT and TD-DFT study of Optical and Electronic Properties of new donor–acceptor–donor (D–A–D') monomers for polymer solar cells. Oxford Open Materials Science*, *3*(1), itad003.

Munusamy, A. P., Ammasi, A., Shajahan, S., Ahamad, T., & Khan, M. M. (2021). *Quantum chemical investigation on D-π-A-*based phenothiazine organic chromophores with spacer and electron acceptor effects for DSSCs. Structural Chemistry*, *32*(6), 2199-2207.

Ndiaye, A., Dioum, A., Oprea, C. I., Dumbrava, A., Lungu, J., Georgescu, A., … Youm, I. (2021). *A Combined Experimental and Computational Study of Chrysanthemin as a Pigment for Dye-Sensitized Solar Cells*. 1–15.

Ossai, A. N., Ezike, S. C., Timtere, P., & Ahmed, A. D. (2021). Enhanced photovoltaic performance of dye-sensitized solar cells-based Carica papaya leaf and black cherry fruit co-sensitizers. *Chemical Physics Impact*, *2*(April), 100024. https://doi.org/10.1016/j.chphi.2021.100024

Pandey, A. K., Kalidasan, B., Kumar, R. R., Rahman, S., Tyagi, V. V, Samykano, M., & Tyagi, S. K. (2022). *Solar Energy Utilization Techniques , Policies , Potentials , Progresses , Challenges and Recommendations in ASEAN Countries*. 1–26.

Păuşescu, I., Todea, A., Dreavă, D. M., Boboescu, T., Paţcan, B., Paţcan, L., ... & Medeleanu, M. (2022). *Experimental and computational studies on bio-inspired flavylium salts as sensitizers for dye-sensitized solar cells. Materials*, *15*(19), 6985.

Sanjay, P., Isaivani, I., Deepa, K., Madhavan, J., & Senthil, S. (2019). The preparation of dye sensitized solar cells using natural dyes extracted from Phytolacca icosandra and Phyllanthus reticulatus with ZnO as photoanode. *Materials Letters*, *244*, 142–146. https://doi.org/10.1016/j.matlet.2019.02.072

Shah, W., Faraz, S. M., Arshad, S., Haider, S. S., & Sayyad, M. H. (2023). *Co-Sensitized DSSC with Natural Dyes Extracted from Beetroot , Pomegranate and Cranberry †*. 2–7.

Sharma, K., Sharma, V., & Sharma, S. S. (2018). *Dye-Sensitized Solar Cells : Fundamentals and Current Status*. 6.

Sreeja, S., & Pesala, B. (2018). Co - sensitization aided efficiency enhancement in betanin – chlorophyll solar cell. *Materials for*

Renewable and Sustainable Energy, 7(4), 1–14. https://doi.org/10.1007/s40243-018-0132-x

Subbarao, M. (2023). *New organic dyes based on D - π - A structural sensitiz - ers for Dye-sensitized solar cells (DSSC ' s): DFT and TD-DFT investigation . 17*(JUly), 1060–1073. https://doi.org/10.5530/ctbp.2023.3.44

Syafinar, R., Gomesh, N., Irwanto, M., Fareq, M., & Irwan, Y. M. (2015). Chlorophyll Pigments as Nature Based Dye for Dye-Sensitized Solar Cell (DSSC). In *Energy Procedia* (Vol. 79). Elsevier B.V. https://doi.org/10.1016/j.egypro.2015.11.584

Vuai, S. A. H., Khalfan, M. S., & Babu, N. S. (2021). Heliyon DFT and TD-DFT studies for optoelectronic properties of coumarin based donor- π -acceptor (D- π -A) dyes : applications in dye-sensitized solar. *Heliyon*, *7*(November), e08339. https://doi.org/10.1016/j.heliyon.2021.e08339